Pervaporation of Alcohols in PBT Near the Glass Temperature: An Analysis of the Concentration-Dependent Diffusion

K. HUBER, J. NOWACK, D. GÖRITZ

Universität Regensburg, Institut für Experimentelle und Angewandte Physik, D-93040 Regensburg, Germany

Received 12 June 1997; accepted 4 November 1997

ABSTRACT: Differential pervaporation measurements with alcohols in poly(butylene terephthalate) (PBT) in the range of its glass transition temperature were performed. The applied apparatus is based on a gas-chromatographic detection system. The concentration dependency of the diffusion coefficient prevents solving the diffusion equations analytically. Therefore, a method was developed using finite differences in space and time to obtain numerical permeant fluxes under the assumption of certain concentration dependencies $D(c)$. The results of this procedure were compared with the measured permeant fluxes, and intrinsic diffusion coefficients D_0 and explicit functions $D(c)$ were attained. In addition, the concentration profiles of the liquids in the membrane for all times of the pervaporation process could be displayed. The evaluation of the temperature dependency of $D(c)$ shows maxima for the plastification effect of the alcohol molecules at a temperature near T_g. © 1998 John Wiley & Sons, Inc. J Appl Polym Sci 68: 1503–1515, 1998

Key words: pervaporation; glassy polymer; finite difference method; PBT; concentration-dependent diffusion

INTRODUCTION

The transport of gases and organic vapors in dense polymer membranes is important for theoretical as well as for technological reasons. Besides the application as barrier materials during the last decades, polymers are intensively used for the separation of gas and liquid mixtures.[1–6]

From most of these investigations, it is well known that the diffusion of vapors in glassy polymers is "anomalous", meaning that the process cannot be adequately described by Fick's laws. Reviews of phenomena that may occur in the transport of vapors in glassy polymers were given by Crank and Park[7] and by Frisch.[8] In contrast to polymers above their glass temperature T_g, where only concentration-independent or concentration-dependent diffusion can be observed, glassy polymers show a variety of further phenomena, among them, time-dependent diffusion anomalies, Case II transport behavior, and solvent-induced crazing.[9] The distinction between these phenomena is often done by analysis of the time dependency of the normalized mass uptake of the penetrant during the sorption process. If the mass uptake is proportional to the square root of time, Fickian diffusion is assumed, whereas a linear proportionality suggests a Case II transport as the controlling transport mechanism. More complicated time dependencies indicate coupled processes.[10] However, a closer inspection of the experimental data within the error limits by statistical analysis shows the uncertainty of a clear determination of the time dependency.[11]

Correspondence to: K. Huber.

Contract grant sponsor: Deutsche Forschungsgemeinschaft (DFG); contract grant number: Go 287/21-1.

Journal of Applied Polymer Science, Vol. 68, 1503–1515 (1998)
 CCC 0021-8995/98/091503-13

In the case of concentration-dependent diffusion, the techniques for sorption kinetics can only determine an effective diffusion coefficient. For a variety of glassy polymers and organic vapors, this has been performed.[12,13] By variation of the penetrant activity, further information about the diffusion coefficient can be obtained.[14] But for the determination of a relationship between the diffusion coefficient and concentration, the sorption and desorption method is insufficient, apart from the accuracy of the measurements.[15]

In the pervaporation process, the "feed" liquid or mixture is brought up on one side of the membrane and a fraction of it ("permeate") is evolved in the vapor state on the opposite side, which is kept under a vacuum by continuous pumping or is purged with a stream of carrier gas. The permeate is finally either collected in the liquid state after condensation or analyzed directly by a detector.

The method of differential permeation, in which the transient permeation rate through a membrane is measured as a function of time, is suitable for the determination of the diffusion coefficient and its proper deviations from a constant value. It has several advantages over integral permeation methods ("time-lag" methods) or sorption methods.[16] In this article, a differential permeation method is described, which allows the continuous monitoring of the penetrant passing through the membrane from the moment of its exposure to the liquid until a steady state is reached. By using suitable detectors, this pervaporation device makes it possible to register each singular component of a mixture from water and an organic liquid individually over the whole time of measurement.

Generally, the diffusion coefficient is derived by comparing the experimental permeation rates with an expression representing the solution of Fick's laws with a constant diffusion coefficient. If this does not work due to strong interactions of the permeant molecules with the polymeric material, a concentration dependency of the diffusion coefficient is suspected. In this case, no analytical solutions can be obtained and Fick's laws may be solved numerically.[17,18] Another possibility is the calculation of an apparent diffusion coefficient as a function of time.[19] But none of these methods is suitable to elucidate an analytical function for the concentration dependency of the diffusion coefficient.

Few authors have investigated differential permeation for organic vapors or differential pervaporation for organic liquids in glassy polymers up to now.[20–22] It was shown that the permeation of organic vapors in the limit of low permeant concentration can be described with a concentration-independent diffusion coefficient.[12,23] But no method is known for determining the analytical functions of the concentration dependency of the diffusion coefficient by differential pervaporation in the glassy state besides this limiting behavior.

In this article, a method is presented dealing with finite differences in the coordinates of membrane thickness and the time of the pervaporation process. Starting with the boundary conditions of the experiment at time zero, the concentrations of the permeant are calculated step by step in time and space within the membrane. This is performed with respect to an arithmetic expression for the diffusion coefficient. From this procedure, concentration profiles result, and by using Fick's first law at the downstream surface of the membrane, a differential permeant flux is obtained. This can be compared with a measured permeant flux. In case of agreement, it can be concluded that the expression for the diffusion coefficient was suitable in this case.

Differential pervaporation of various alcohols through membranes of poly(butylene terephthalate) (PBT) in the range of its glass temperature were measured. This polymer is of commercial importance not only in its pure form but also as a blend with other different polymers.[24,25]

The sorption of gases in PBT in this temperature range was already examined.[26–28] Also, permeation measurements of carbon dioxide in PBT blends have been done.[29]

THEORETICAL

Taking Fick's first law in the one-dimensional case (i.e., diffusion through a thin sheet), the permeation flux j is a function of the diffusion coefficient D, which may depend on the concentration c, and the change of concentration c with distance x into the sheet:

$$j = -D(c)\,\frac{\partial c}{\partial x} \tag{1}$$

The change of concentration in a volume of the membrane must equal the difference of the flux in and out of this volume, div j, leading to

$$\frac{\partial c}{\partial t} + \frac{\partial j}{\partial x} = 0 \tag{2}$$

Combining eqs. (1) and (2) results in Fick's second law:

$$\frac{\partial c}{\partial t} = \frac{\partial}{\partial x}\left(D(c)\frac{\partial c}{\partial x}\right) \tag{3}$$

Analytical solutions of eq. (3) can only be obtained for either a constant diffusion coefficient or a concentration-dependent diffusion coefficient under special starting and boundary conditions.[30] In other cases, Fick's laws have to be solved numerically. Some attempts can be found in the literature.[17,30] Another possibility is the application of finite difference methods. Vergnaud et al.[31,32] developed several numerical schemes using these methods to calculate the concentration profiles of liquids during sorption processes within membrane materials. In this work, their methods were transferred to obtain curves of the permeation flux for different terms of the concentration dependency of the diffusion coefficient. These computed curves can then be compared with our measurements to obtain various information.

The thickness of the sheet is divided into finite increments in space, Δx. We used 20 slices. Higher numbers of slices did not affect the results anymore. Furthermore, the time is split into finite increments, Δt. The time, t, and the place, x, of the progression of the molecules in the membrane are defined as follows:

$$t = i\Delta t \quad \text{and} \quad x = n\Delta x$$

with n and i being integers. Applying this procedure, a two-dimension space–time diagram with elements $c_{n,i}$ results. Let us now consider a volume V of the membrane described by a cross-sectional area, S, and a thickness, Δx. The direction of the permeant flux shall be perpendicular to the cross section, the entering section being denoted by a, and the opposite section, by b. From eq. (2) follows[31]

$$S\left[-D_a\left(\frac{\partial c}{\partial x}\right)_a + D_b\left(\frac{\partial c}{\partial x}\right)_b\right]\Delta t = (S\Delta x)(c_{n,i+1} - c_{n,i}) \tag{4}$$

$c_{n,i+1}$, $c_{n,i}$ being the concentrations in slice n at time $i + 1$ and i. The concentration gradients are approximated by the chord slope between positions Δx apart:

$$-\left(\frac{\partial c}{\partial x}\right)_a = \frac{c_{n-1,i} - c_{n,i}}{\Delta x} \quad \text{and}$$

$$-\left(\frac{\partial c}{\partial x}\right)_b = \frac{c_{n,i} - c_{n+1,i}}{\Delta x} \tag{5}$$

D_a and D_b are replaced by the following expressions:

$$D_a = D_0 f\left(\frac{c_{n-1,i} + c_{n,i}}{2}\right) \quad \text{and}$$

$$D_b = D_0 f\left(\frac{c_{n,i} + c_{n+1,i}}{2}\right) \tag{6}$$

where D_0 is the intrinsic diffusion coefficient for concentrations $c \to 0$. The function f expresses the concentration dependency of the diffusion coefficient. Using the dimensionless parameter G,

$$G = \frac{D_0\Delta t}{(\Delta x)^2} \tag{7}$$

the basic equation becomes

$$c_{n,i+1} = c_{n,i} + G\left[f\left(\frac{c_{n-1,i} + c_{n,i}}{2}\right)(c_{n-1,i} - c_{n,i}) - f\left(\frac{c_{n,i} + c_{n+1,i}}{2}\right)(c_{n,i} - c_{n+1,i})\right] \tag{8}$$

The boundary conditions for a differential permeation experiment within this notation are

$$c_{n,i} = 0 \quad n > 0 \quad i = 0$$
$$c_{n,i} = c_s \quad n = 0 \quad \forall i$$
$$c_{n,i} = 0 \quad n = 20 \quad \forall i$$

with the equilibrium solubility c_s. Given these starting conditions and an expression for the diffusion coefficient

$$D(c) = D_0 f(c) \tag{9}$$

each point in the space–time diagram can be cal-

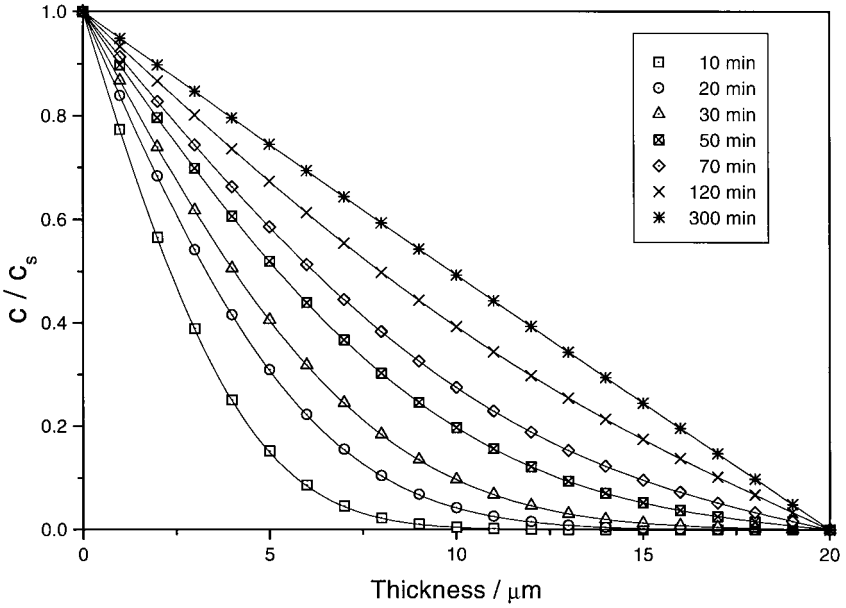

Figure 1 Comparison of numerically determined (symbols) and analytically calculated (lines) concentration profiles in a membrane with $D_0 = 1 \cdot 10^{-10}$ cm^2/s.

culated. To test the method, concentration profiles for a constant diffusion coefficient are shown in Figure 1 and compared to curves of the analytical solution taken from the literature.[30] The good agreement between the numerical and the analytical profiles is obvious.

Different mathematical expressions are used in the literature for the concentration dependency of the diffusion coefficient. Widely applied in solvent transport through polymer membranes above the glass temperature is [5]

$$D(c) = D_0 \exp(\gamma c) \qquad (10)$$

with γ the plastification coefficient. Taking eq. (10), the concentration profile in the steady state of pervaporation can be evaluated by suitable integration of Fick's first law eq. (1)[5]:

$$c(x) = \frac{1}{\gamma} \ln\left\{\frac{x}{d}\left[1 - \exp(\gamma c_s)\right] + \exp(\gamma c_s)\right\}$$

$$\text{with} \quad 0 \le x \le d \qquad (11)$$

Another expression often employed is a linear term:

$$D(c) = D_0(1 + ac) \qquad (12)$$

In this case, the analytical steady-state profile reads

$$c(x) = \left(\frac{2}{a}\left(c_s + \frac{a}{2}c_s^2\right)\left(1 - \frac{x}{d}\right) + \frac{1}{a^2}\right)^{1/2} - \frac{1}{a}$$

$$\text{with} \quad 0 \le x \le d. \qquad (13)$$

Figure 2 shows a comparison of the numerically calculated steady-state concentration profiles with the analytical results according to the above equations. As in the case of a constant diffusion coefficient, a good agreement between both methods is found.

But the aim of our numerical method was not just the calculation of concentration profiles but, above all, to gain knowledge of the generally unknown function $D(c)$. The permeant flux can be obtained by applying Fick's first law at the "downstream boundary" of the space–time-diagram:

$$j(i\Delta t) = D_0 \frac{c_{19,i}}{\Delta x} \qquad (14)$$

because the concentration at the downstream side of the membrane is zero for all times.

In Figure 3, numerically generated permeant curves for a concentration dependency according to

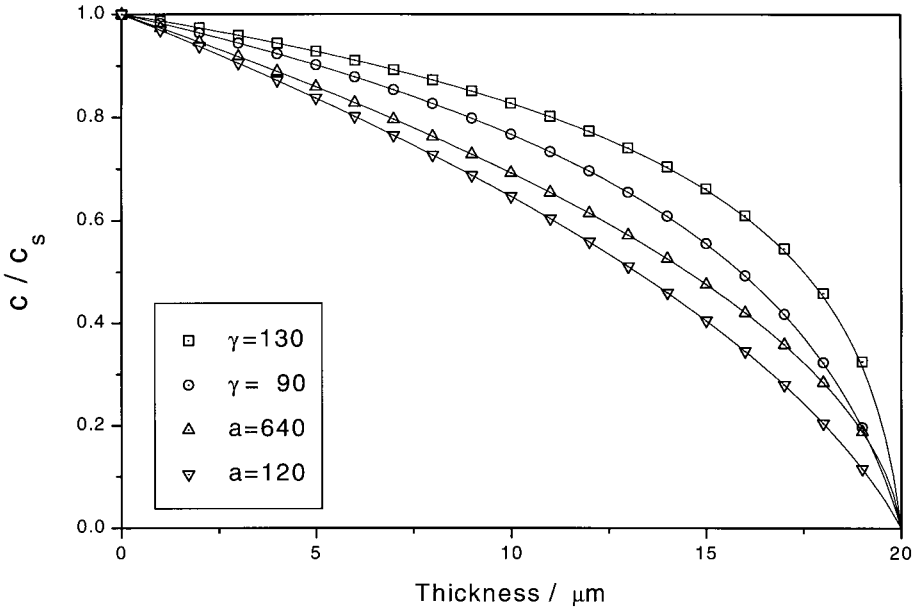

Figure 2 Comparison of numerically determined (symbols) and analytically calculated (lines) steady-state concentration profiles in a membrane with different functions $D(c)$.

eq. (10) are plotted. For $\gamma c_s = 0$, the result matches the solution of Fick's second law for a concentration-independent diffusion coefficient.[19,30]

The curves presented in Figure 3 depend on the product of γ times c_s, c_s being the equilibrium solubility. Thus, to obtain the parameter γ, the solubility c_s has to be determined independently. The data are normalized to the steady-state flux j_s reached at long time. A normalized, measured permeant curve can then be compared with this set of numerical curves. If the measured curve exactly matches a numerical one, it can be stated that the numerical curve represents a correct concentration dependency. Hence, the plastification

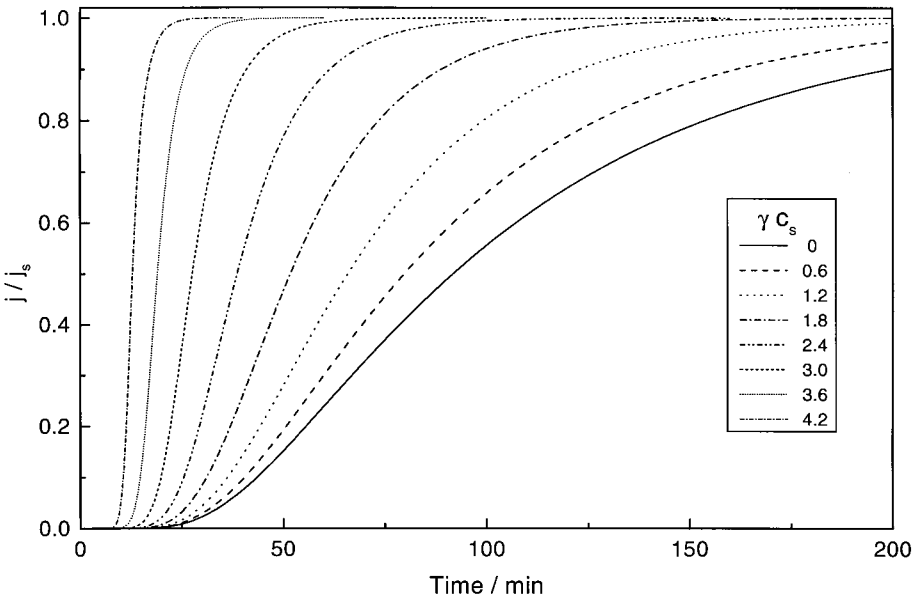

Figure 3 Numerical permeant fluxes for $D(c) = D_0\exp(\gamma c)$ with different values for the product γc_s.

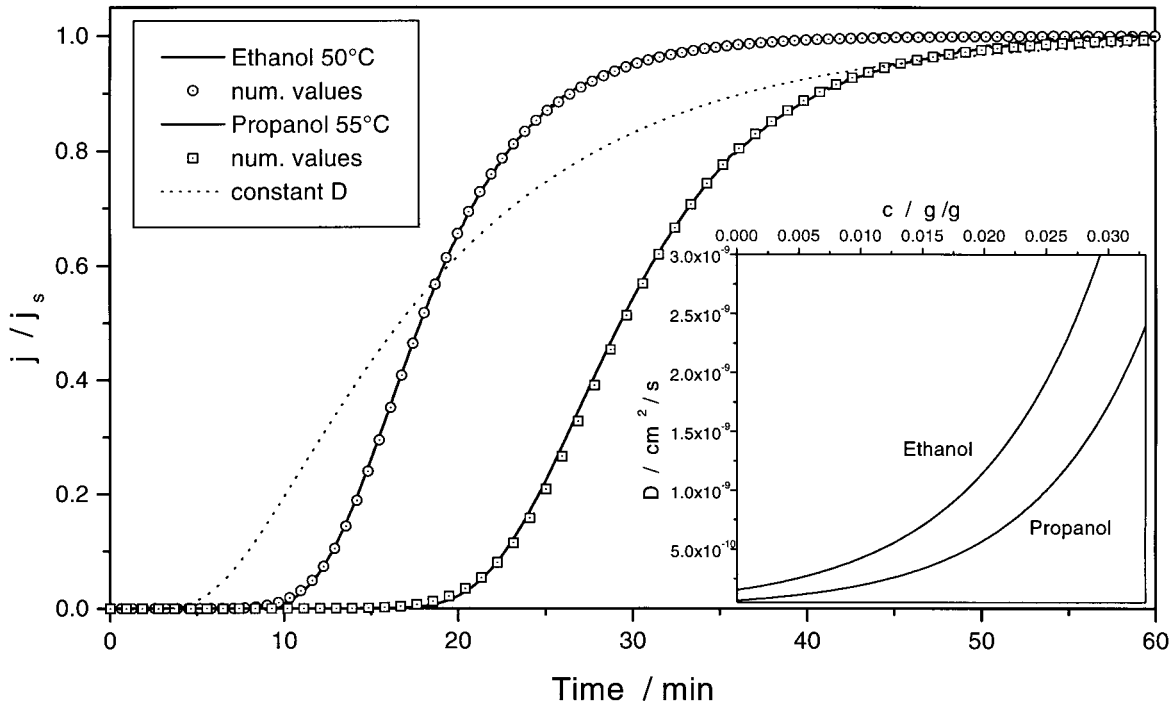

Figure 4 Comparison of normalized measured permeant fluxes of alcohols through PBT with numerically generated permeant fluxes with concentration-dependent diffusion coefficient $D(c) = D_0\exp(\gamma c)$.

parameter γ and the intrinsic diffusion coefficient D_0 are determined. To match the two curves, it is necessary to scale the time axis of one curve. This is permitted when changing the intrinsic diffusion coefficient according to the product $D_0 \cdot \Delta t$, a fixed, dimensionless number within the numerical process [eq. (8)]. If a matching is not possible, the conclusion has to be drawn that the used expression for the concentration dependency is not valid for this single experiment. For an example, Figure 4 shows the result of the described procedure for the permeant curves of ethanol measured at temperature 50°C and propanol at temperature 55°C. For reasons of comparison, the best fit with a constant D for the permeant curve of ethanol is also shown. The good agreement of the experimental and numerical curves is evident. It suggests that the pervaporation process of these alcohols at temperatures above the T_g is concentration-dependent with an expression like eq. (10). The values obtained with this numerical procedure are $\gamma c_s = 3$ for the ethanol and $\gamma c_s = 3.6$ for the propanol curve. The insert of Figure 4 displays the explicit function $D(c)$. Knowing this, it is feasible to present concentration profiles in the membrane at different times of the pervaporation process (Fig. 5).

EXPERIMENTAL

Material

The measurements were done with membranes of Ultradur 4550 from BASF AG (Ludwigshafen, Germany) without any additives. The density determined by the gradient method was $\rho = 1.293$ g/cm^3. Using values from the literature for amorphous ($\rho_a = 1.280$ g/cm^3)[33] and crystalline ($\rho_c = 1.43$ g/cm^3)[34] PBT, this corresponds to a degree of crystallinity of about 10%. The glass transition temperature T_g resolved with a Perkin–Elmer DSC 2 instrument was 322 K. The sample thickness for pervaporation measurements was 20 μm.

Solubility Measurement

Different pieces of the membrane material with a thickness of 100 μm were immersed into various alcohols at appropriate temperatures. Upon removal, the samples were blotted on filter paper to remove excess liquid from the surface and weighed. Equilibrium sorption was assumed when no further weight change could be detected. The solubility of a certain alcohol is achieved from

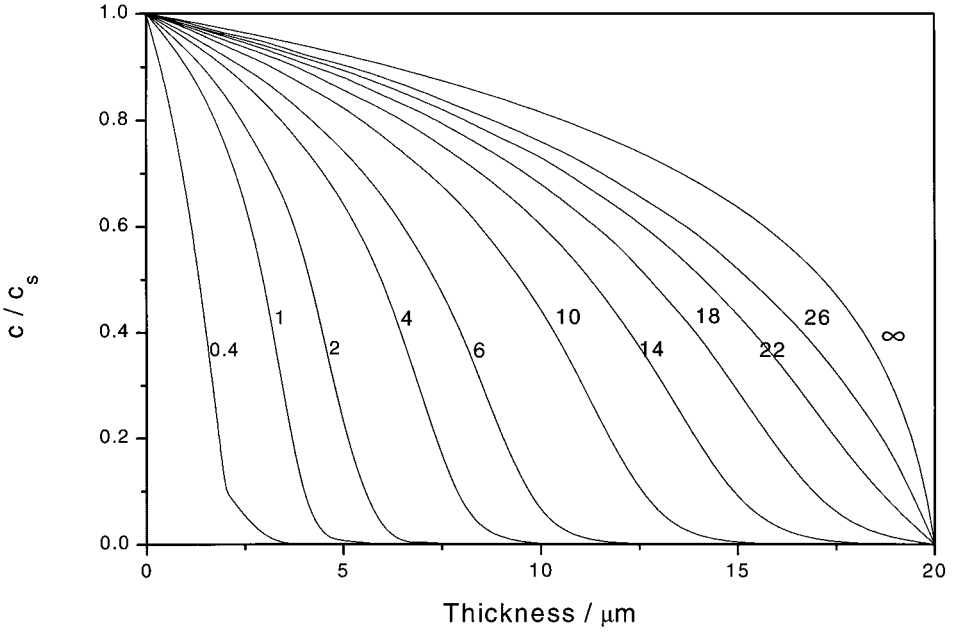

Figure 5 Concentration profiles in the membrane for $\gamma c_s = 3.6$ and $D_0 = 1 \cdot 10^{-10}$ cm^2/s. The numbers at the curves denote the time in min.

$$c_s = \frac{W_\infty - W_0}{W_0} \qquad (15)$$

in units of $g_{\text{liquid}}/g_{\text{polymer}}$, with W_0 and W_∞ the weights at the beginning and in the equilibrium state, respectively.

Pervaporation Apparatus

The pervaporation apparatus was described earlier.[35] A pervaporation cell consisting of stainless steel is divided into two parts: the upstream and downstream volumes. Between these, the probe is placed, supported by a metallic plate with holes. The effective surface area of the membrane in the cell is 8.9 cm^2. The pervaporation cell with the membrane inside is heated in the oven of a gas chromatograph (Model CP 9000, Chrompack) up to the measuring temperature. A helium carrier-gas stream with a constant flow permanently sweeps the downstream volume of the cell. At the beginning of the measurement, the heated liquid is pumped into the upstream volume and the liquid molecules dissolve in the membrane, diffuse through it, and are evaporated into the downstream part of the cell. They are transported by the helium stream to the gas chromatographic detector system consisting of a flame ionization detector (FID) and a thermal conductivity detector (TCD). The detector signal is registered as a function of time by a computer. While the FID exclusively responds to organic compounds, all vapors and gases can be recorded with the TCD. By passing the TCD, the molecules will not be altered, while they are destroyed when registered by the FID. The two detectors can be used singly or both together in a line depending on need. For the measurements presented here, only the FID was taken. Using both detectors during the pervaporation of a liquid mixture consisting of an organic (e.g., alcohol) and a water component, it is possible to monitor the permeation fluxes of both components independently. This has been done for mixtures of alcohols and water and the results will be presented in another article.[36] Calibration of the apparatus is performed in the following way: Instead of the polymer membrane, a metallic plate is placed in the cell. An exact volume of the feed liquid is filled into the gas chromatograph injector by a microsyringe. The corresponding detector signal is recorded and integrated by a computer. During the measurement, it must assured that the detectors work in their range of linearity and that the flow of the carrier-gas stream remains constant.

RESULTS AND DISCUSSION

Solubility

The determined solubilities of the alcohols are shown in Figure 6 in an Arrhenius plot. Within

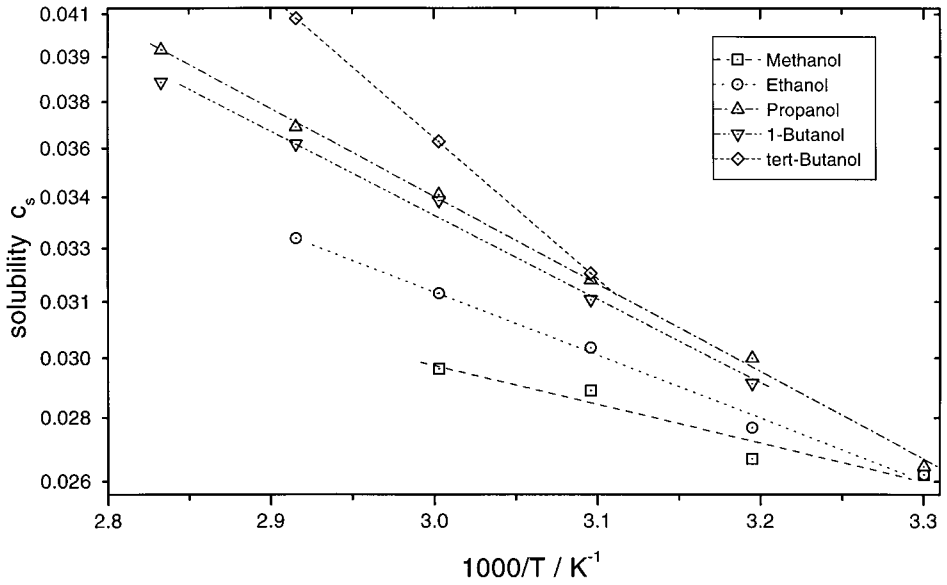

Figure 6 Arrhenius plot of alcohol solubilities in PBT.

the error limits of the measurements, the data satisfy the Arrhenius equation

$$c_s = c_s^{\infty} \exp(-H_s/RT) \qquad (16)$$

where H_s is the heat of sorption, and R, the gas constant. The values obtained for H_s with least-square fits are presented in Table I, and that for c_s^{∞}, in Table II. As mentioned above, the solubilities are given in weight fractions. When plotted against the mol fraction, it can be seen that the smaller the molecules (methanol) the more that are dissolved. The heat of sorption increases with increasing size of the molecule. The values are all positive in contrast to the sorption of carbon dioxide with a value of −10.5 kJ/mol.[26] As the heat of sorption results from the positive enthalpy of mixing and the negative heat of condensation, the positive values of H_s in this work must be attributed to the contribution of mixing. Due to the low solubility values found, neither macroscopic swelling nor solvent-induced crystallization could be observed in the saturated probes.

Concentration-Dependent Diffusion

The pervaporation was measured by applying the method described above in the second section. The intrinsic diffusion coefficients D_0 and the products γc_s for different alcohols were determined at various temperatures. With the solubilities known from above, the plastification parameter γ was evaluated. The results show that at temperatures above 40°C the concentration dependency is well described by eq. (10). Below 40°C, no general expression could be found for the concentration dependency. A detailed examination of the measurements with methanol in the glassy state of PBT,

Table I Heat of Sorption and Activation Energies of the Intrinsic Diffusion Coefficient and Permeation Coefficient for Various Alcohols in PBT in the Range of Its Glass Temperature

		E_{D_0} (kJ/mol)		E_P (kJ/mol)	
Alcohol	H_s (kJ/mol)	$T > T_g$	$T < T_g$	$T > T_g$	$T < T_g$
Methanol	3	70		67	90
Ethanol	5	84	95	103	130
Propanol	7	113	124	106	140
1-Butanol	7	95	134	106	170
tert-Butanol	11	129	200	158	193

Table II Preexponential Factors of Arrhenius Equations for Solubility, Intrinsic Diffusion Coefficient, and Permeation Coefficient for Various Alcohols in PBT in the Range of Its Glass Temperature

Alcohol	c_s^∞ (g/g)	D_0^∞ (cm^2/s)		P^∞ (cm cm^3/cm^{2}s)	
		$T > T_g$	$T < T_g$	$T > T_g$	$T < T_g$
Methanol	0.08	$3.7 \cdot 10^2$		$1.5 \cdot 10^2$	$6.9 \cdot 10^5$
Ethanol	0.21	$7.4 \cdot 10^3$	$4.5 \cdot 10^5$	$1.5 \cdot 10^7$	$3.4 \cdot 10^{11}$
Propanol	0.37	$6.5 \cdot 10^7$	$3.7 \cdot 10^9$	$1.7 \cdot 10^7$	$4 \cdot 10^{12}$
1-Butanol	0.42	$6.3 \cdot 10^5$	$8.2 \cdot 10^{10}$	$9.5 \cdot 10^6$	$9.9 \cdot 10^{16}$
tert-Butanol	2.12	$2.3 \cdot 10^9$	$4.2 \cdot 10^{20}$	$2.9 \cdot 10^{14}$	$7.7 \cdot 10^{19}$

temperature range 25–35°C, through variation of the function for $D(c)$ yields concentration dependencies as shown in Figure 7. The curve for 25°C is very similar to the results in the dual-sorption model for the sorption of gases in polymer glasses.[4] The dual-sorption model states that a part of the dissolved molecules is kept fixed in microcavities. Thus, this part of the molecules cannot plasticize the sample in the same way as do the mobile molecules. This ineffective portion becomes smaller with increasing temperature due to the higher mobility of the polymer chains, leading to an instability of the microcavities. Above a certain temperature, all molecules diffuse in the same way and the concentration dependency is similar to that beyond the glass temperature. This picture easily explains the rest of Figure 7.

The intrinsic diffusion coefficients determined with our method are presented in Figure 8. The reduction of the values with increasing size of the molecules is obvious. Due to its divergent molecular shape, the behavior of *tert*-butanol differs from that of the others. In contrast to the more linear shape of the primary alcohols, the shape of *tert*-butanol is more spherical, leading to an intrinsic diffusion coefficient about one magnitude smaller than that for 1-butanol. This tendency was observed both for glassy and elastomeric polymers in other works.[12,37]

The lines in Figure 8 obtained from a fitting procedure are in agreement with an Arrhenius equation of the following form:

$$D_0 = D_0^\infty \exp(-E_{D_0}/RT) \qquad (17)$$

with E_{D_0} the activation energy of the intrinsic diffusion coefficient and D_0^∞ a preexponential factor. The corresponding results for E_{D_0} are shown in Table I. Also, the preexponential factors are tabulated (Table II) for completeness, in case the reader may need them for empirical correlations

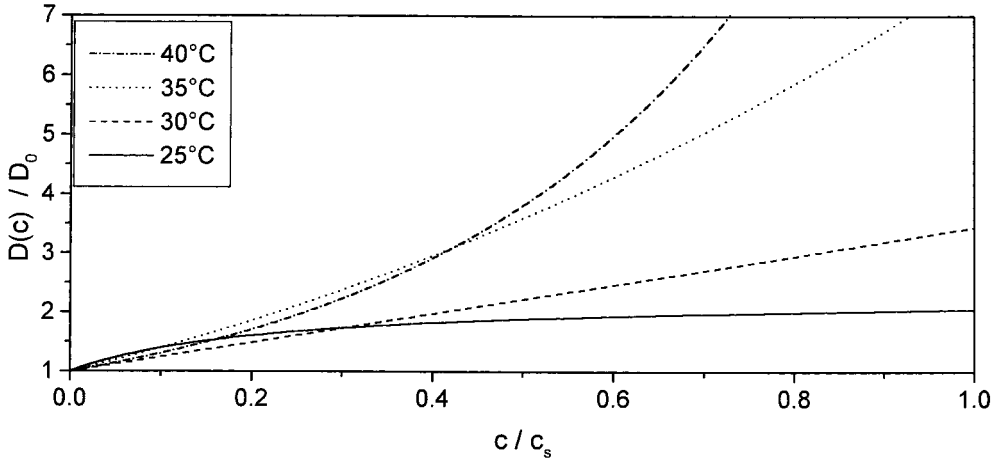

Figure 7 Dependency of the diffusion coefficient from concentration for methanol in the glassy state of PBT.

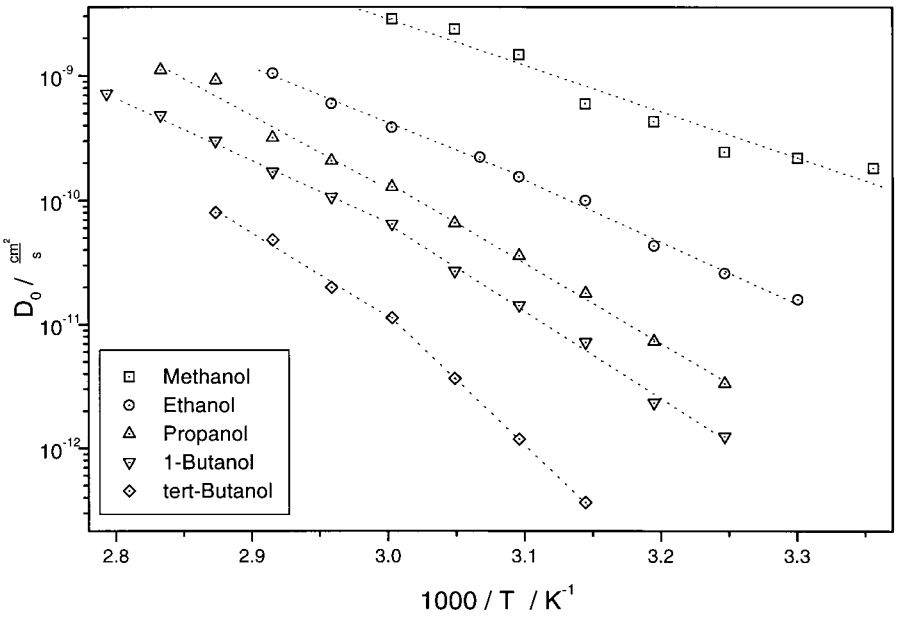

Figure 8 Arrhenius plot of intrinsic diffusion coefficients of alcohols in PBT.

between $\log(D_0^{\infty})$ and E_{D_0} as in refs. 38 and 39. With increasing size of the molecules, the activation energies also increase. Also, a break in the activation energy near the T_g in Figure 8 can be seen increasing with the size of the molecules. Zhou[40] investigated the permeation of gases in PBT in the same temperature range and found a pronounced break in the activation energies for the diffusion coefficient. In contrast to our presented data, the activation energies of the gases were larger above than below the T_g. The same behavior in the vicinity of the T_g was also detected for the permeation of gases in poly(ethylene terephthalate), which is very similar to PBT in its chemical structure, and many other glassy polymers.[41,42] These deviations cannot be explained by the concentration dependency, since D_0 is the intrinsic diffusion coefficient at zero concentration. But a closer inspection of the values obtained by Zhou[40] reveals that with increasing size of the molecules (He, Ar, Ne) the difference in the activation energies below and above the T_g becomes smaller. Also, the other measurements mentioned above were performed with gases, whose molecular size is small compared to the alcohols. Hence, we attribute the changed behavior to the larger size of our penetrating molecules.

In the literature, a comparison of the intrinsic diffusion coefficient D_0 with Crank's mean diffusion coefficient[30]

$$\bar{D} = \frac{1}{c_s}\int_0^{c_s} D(c)\,dc \qquad (18)$$

is often used to visualize the plastification effect. After integration, taking eq. (10) for $D(c)$, it reads

$$\frac{\bar{D}}{D_0} = \frac{1}{\gamma c_s}\left[\exp(\gamma c_s) - 1\right] \qquad (19)$$

This relationship is calculated and presented in Figure 9 versus the temperature for the examined alcohols even in the cases where eq. (10) is not fulfilled. The factor γc_s in eq. (19) ranges from 1.5 to 3.9 for the values shown in Figure 9. It is easily recognized for each alcohol that the plastification effect reaches a maximum around the T_g. The position of the maxima seems to move with increasing molecular size to higher temperatures and correlates with the position of the breaks of the activation energies in Figure 8. It is well known that the glass transition extends over a finite temperature range with a typical width in the order of 10°.[43] On the other hand, the interaction between the polymer and the penetrant may reduce the temperature at which the glass transition is observed.[44,45]

A possible interpretation of these maxima can be outlined via the analysis of the chain mobility in the region of the T_g. Below the T_g, the alcohol

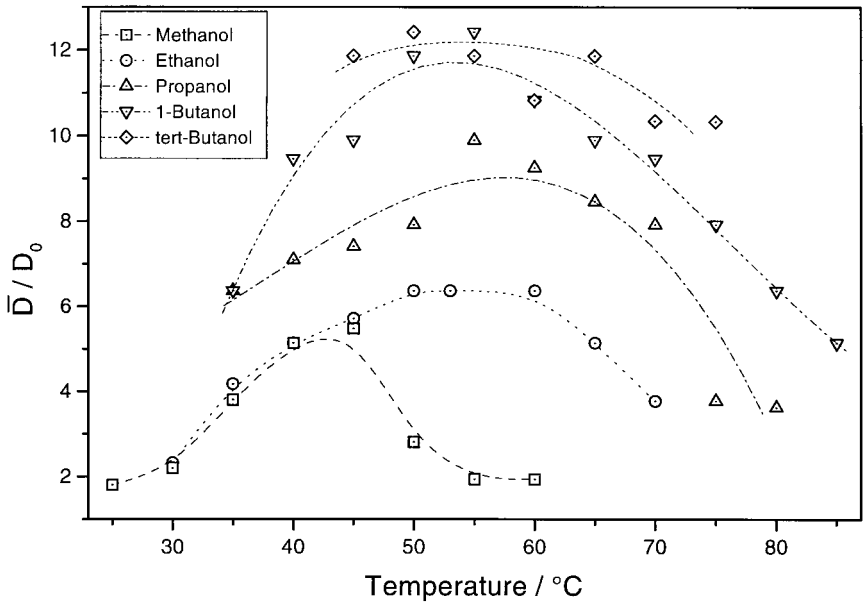

Figure 9 $\bar{D}/D_0$ versus temperature showing the plastification effect of the alcohols in PBT.

molecules are not able to produce a plasticizing effect due to the restricted chain mobility. Near the T_g, the increased mobility is sufficiently high for small molecules to plasticize the polymer membrane. For larger molecules, the corresponding temperature has to be higher due to their molecular volume. Hence, the break of the activation energies lies above the T_g. Distinctly further above the T_g, the mobility of the chains is increased to such an extent that the additional plasticizing effect of the alcohol molecules is of minor importance. Note that the plastification effect is stronger for the bigger molecules. In the Hildebrand solubility parameter concept, a larger interaction between a polymer and a liquid is assumed when the difference of their solubility parameters is small.[46] With a solubility parameter $\delta_{\mathrm{PBT}} = 20.5$ $(\mathrm{J/cm^3})^{1/2}$ for PBT[47] and values from the literature for the alcohols [$\delta_{tert\text{-butanol}} = 21.7$ $(\mathrm{J/cm^3})^{1/2}$ to $\delta_{\mathrm{methanol}} = 29.7$ $(\mathrm{J/cm^3})^{1/2}$],[46] the maxima in Figure 9 increase in the same order as the differences of the solubility parameters decrease.

Permeability Coefficient

From the steady-state signal of the permeant flux j_s, the permeability coefficient P is gained from

$$P = j_s d \tag{20}$$

with d the membrane thickness. The temperature dependency of the permeability coefficients (Fig. 10) shows a quite similar behavior to that of the intrinsic diffusion coefficients. The results for the activation energies E_P for permeation obtained from fits with an Arrhenius equation

$$P = P^{\infty}\exp(-E_P/RT) \tag{21}$$

are listed in Table I. The resulting values for P^{∞} are presented in Table II. The change of the activation energies at temperatures in the region of the T_g is even more pronounced. Due to the considerable temperature dependency of the permeability coefficients (e.g., an increase of three orders of magnitude was observed in a temperature interval of 35°C for 1-butanol), high activation energies result.

Similar high activation energies of the diffusion of alcohols were observed in studying the sorption kinetics of poly(methyl methacrylate) sheets in the range of its T_g by Nicolais et al.[10] However, Case II diffusion was observed in these investigations, the mass uptake being directly proportional to time. In our examinations, not only the mass uptake in the steady state was registered but at all intermediate points. Even in the cases of high plastification parameters γ, the mass uptake took place with respect to the square root of time. No other indications for Case II diffusion were found. Hence, our measurements seem to be clearly not of Case II diffusion type.

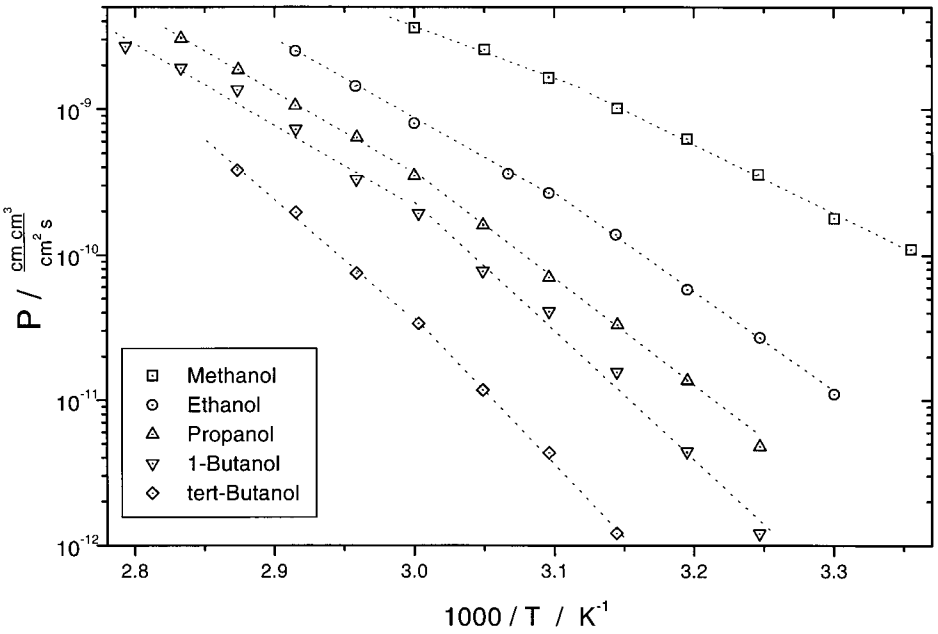

Figure 10 Arrhenius plot of the permeability coefficients of alcohols in PBT.

CONCLUSION

In this article, we presented a detailed analysis of the differential pervaporation of alcohols through poly(butylene terephthalate) membranes in the range of its glass temperature. The interpretation of these measurements cannot be performed using standard methods because of the concentration dependency of the diffusion coefficient $D(c)$. Thus, a finite difference method was introduced, permitting one to obtain information on the intrinsic diffusion coefficient D_0 and the expression $D(c)$. This was done by comparing numerical calculated permeant fluxes with experimental measured ones. Furthermore, concentration profiles were presented for all times of the pervaporation process. Activation energies for the intrinsic diffusion coefficients D_0, the permeation coefficients P, and the heat of sorption H_S were calculated. Due to the molecule size of higher alcohols, these activation energies increase up to 200 kJ/mol, but no indications for Case II diffusion were found. The activation energies differ for temperatures below and above the glass transition. Contrary to the literature values for gases, the activation energies above are lower than below. With the information gained with our method, it was possible to visualize the temperature dependency of the plastification effect of the alcohols in the membrane. Maxima appear in the vicinity of the T_g shifted to higher temperatures with larger molecules.

The authors are grateful to BASF, Ludwigshafen, for the PBT samples. The authors appreciate the fruitful discussions with Dr. S. Kreitmeier. Moreover, one of the authors (K. H.) thanks the Deutsche Forschungsgemeinschaft (DFG) for financial support (Go 287/21-1).

REFERENCES

1. N. Toshima, Ed., *Polymers for Gas Separation,* VCH, New York, 1992.
2. J. G. A. Bitter, *Transport Mechanisms in Membrane Separation Processes,* Plenum Press, New York, 1991.
3. M. Mulder, *Basic Principles of Membrane Technology,* Kluwer, Dordrecht, The Netherlands, 1991.
4. W. J. Koros, Ed., *Barrier Polymers and Structures,* ACS Symposium Series, American Chemical Society, Washington, DC, 1990.
5. R. Y. M. Huang, Ed., *Pervaporation Membrane Separation Process,* Elsevier, Amsterdam, 1991.
6. R. D. Noble and S. A. Stern, Eds., *Membrane Separations Technology,* Elsevier, Amsterdam, 1995.
7. J. Crank and G. S. Park, *Diffusion in Polymers,* Academic Press, London, New York, 1968.
8. H. L. Frisch, *Polym. Eng. Sci.,* **20,** 2 (1980).
9. H. B. Hopfenberg and H. L. Frisch, *J. Polym. Sci. Part B Polym. Lett.,* **7,** 405 (1969).
10. L. Nicolais, E. Drioli, and H. B. Hopfenberg, *J. Membr. Sci.,* **3,** 231 (1978).
11. G. W. Sinclair and N. A. Peppas, *J. Membr. Sci.,* **17,** 329 (1984).

12. A. R. Berens and H. B. Hopfenberg, *J. Membr. Sci.,* **10,** 283 (1982).
13. S. Pauly, in *Polymer Handbook,* 3rd ed., J. Brandrup and E. H. Immergut, Eds., Wiley-Interscience, New York, 1989.
14. L. Bove, C. D'Aniello, G. Gorassi, L. Guadagno, and V. Vittoria, *J. Appl. Polym. Sci.,* **62,** 1035 (1996).
15. C. K. Yeom and R. Y. M. Huang, *J. Membr. Sci.,* **68,** 11 (1992).
16. R. M. Felder, *J. Membr. Sci.,* **3,** 15 (1978).
17. J. B. Brolly, D. I. Bower, and I. M. Ward, *J. Polym. Sci. Polym. Phys.,* **34,** 761 (1996).
18. Q. T. Nguyen, R. Gref, R. Clement, and H. Lenda, *Colloid Polym. Sci.,* **271,** 1134 (1993).
19. X. Q. Nguyen, M. Sipek, and Q. T. Nguyen, *Polymer,* **33,** 3698 (1992).
20. N. Yi-Yan, R. M. Felder, and W. J. Koros, *J. Appl. Polym. Sci.,* **25,** 1755 (1980).
21. T. Duncan, W. J. Koros, and R. M. Felder, *J. Appl. Polym. Sci.,* **28,** 209 (1983).
22. H. Eustache and G. Histi, *J. Membr. Sci.,* **8,** 105 (1981).
23. S. P. Chen and J. A. D. Edin, *Polym. Eng. Sci.,* **20,** 40 (1980).
24. D. Delimoy, B. Goffaux, J. Devaux, and R. Legras, *Polymer,* **36,** 3235 (1995).
25. Y. Y. Cheng, M. Brillhart, P. Cebe, and M. Capel, *J. Polym. Sci. Part B Polym. Phys.,* **34,** 2953 (1996).
26. L. Phan Thuy and J. Springer, *Colloid Polym. Sci.,* **266,** 614 (1988).
27. Z. Zhou and J. Springer, *J. Appl. Polym. Sci.,* **47,** 7 (1993).
28. Z. Zhou, J. D. Schultze, and J. Springer, *J. Appl. Polym. Sci.,* **47,** 13 (1993).
29. S. Chin, T. Gaskins, and C. J. Durning, *J. Polym. Sci. Part B Polym. Phys.,* **34,** 2689 (1996).
30. J. Crank, *The Mathematics of Diffusion,* 2nd ed., Clarendon Press, Oxford, 1975.
31. J. M. Vergnaud, *Liquid Transport Processes in Polymeric Materials,* Prentice-Hall, Englewood Cliffs, NJ, 1991.
32. T. M. Aminabhavi, H. T. S. Phayde, J. D. Ortego, and J. M. Vergnaud, *Polymer,* **37,** 1677 (1996).
33. E. P. Chang and E. L. Slagowski, *J. Appl. Polym. Sci.,* **22,** 769 (1978).
34. U. Alter and R. Bonart, *Colloid Polym. Sci.,* **254,** 348 (1976).
35. T. Walcher and D. Göritz, *Macromol. Chem. Phys.,* **196,** 429 (1995).
36. K. Huber and D. Göritz, to appear.
37. K. W. Böddecker, G. Bengston, and H. Pingel, *J. Membr. Sci.,* **54,** 1 (1990).
38. W. J. Koros, *Barrier Polymers and Structures,* ACS Symposium Series, *American Chemical Society,* Washington, DC, 1990.
39. D. W. van Krevelen, *Properties of Polymers,* Elsevier, Amsterdam, 1990.
40. Z. Zhou, Dissertation, TU Berlin, 1991.
41. A. S. Michaels, W. R. Vieth, and J. A. Barrie, *J. Appl. Phys.,* **34,** 13 (1963).
42. G. Strobl, *The Physics of Polymers,* Springer-Verlag, Berlin, 1996.
43. R. Gavara, R. Catala, S. Aucejo, D. Cabedo, and R. Hernandez, *J. Polym. Sci. Part B Polym. Phys.,* **34,** 1907 (1996).
44. M. Samus and G. Rossi, *Macromolecules,* **29,** 2275 (1996).
45. R. N. Haward, Ed., *The Physics of Glassy Polymers,* Applied Science, London, 1973.
46. E. A. Grulke, in *Polymer Handbook,* 3rd ed., J. Brandrup and E. H. Immergut, Eds., Wiley-Interscience, New York, 1989.
47. J. Devaux, Université Catholique de Louvian, Belgium, private communication.